Adjoint-state method applied to kinematic source inversion:

From a benchmark to a real earthquake

Sanchez-Reyes H. S.[1]
with Tago J.[2], Métivier L.[1,3], Cruz-Atienza V. M.[4] and Virieux J.[1]
Friday 28th April, 2017

1. Institut des Sciences de la Terre, UGA, France
2. Facultad de Ingeniría, UNAM, Mexico
3. Laboratoire Jean Kuntzmann, UGA, France
4. Instituto de Geofísica, UNAM, Mexico

Outline

Outline

Introduction

Theory: Adjoint-state method for kinematic source inversion

Exercise 1: Source Inversion Validation (SIV1)

Exercise 2: 2016 Kumamoto earthquake

Further investigation: progressive window-time inversion

Perspectives and Conclusions

Kinematic source model?

Earthquake:	Sudden release of energy (partly transformed into waves).
Stress relaxation:	Dynamic source model (rupture physics).
Shear slip on fault:	Kinematic source model (seismograms computation).

Our problem: kinematic inversion?

On a discrete fault plane, find the spatio-temporel evolution of the slip during the seismic rupture.

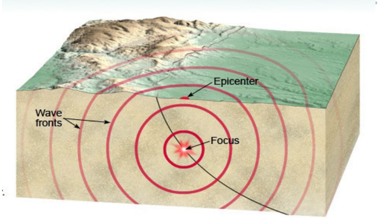

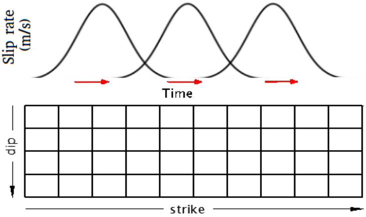

On the shelf, precomputed stress-state kernel $\mathcal{T}_{ni}$ from Green's functions in a known velocity medium from fault points to receiver positions

$$\mathcal{T}_{ni}(\underline{x}, t-\tau; \underline{\xi}, 0) = \sum_m \mu(\underline{\xi}) \left[G_{ni,m}(\underline{x}, t-\tau; \underline{\xi}, 0) + G_{nm,i}(\underline{x}, t-\tau; \underline{\xi}, 0) \right] \eta_m .$$

1. Model: slip-rate vector $\underline{V}_T(\underline{\xi}, t)$ at fault position $\underline{\xi}$ for time t.
2. Data: particle velocity $\underline{v}(\underline{x}, t)$ at # receivers through a simple integral

$$v_n(\underline{x}, t) = \sum_i \int_{t_1}^{t_2} d\tau \int\int_{\underline{\xi}} V_{T_i}(\underline{\xi}, \tau) \mathcal{T}_{ni}(\underline{\xi}, t-\tau; \underline{x}, 0) d\underline{\xi}.$$

$$(n \in \{1,2,3\} \text{ and } i \in \{1,2\})$$

from representation theorem (Aki and Richards, 2002)

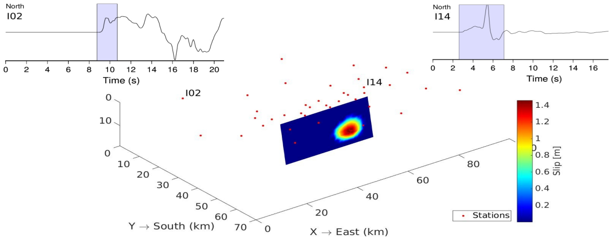

Synthetic windowed seismograms computed from a rupture time interval.

Model reduction: Linear vs Non-linear formulations

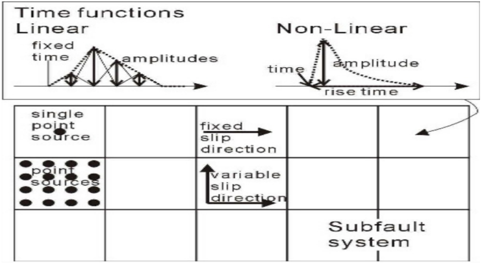

Typical subfault parameterizations
(from Ide et al. 2005)

Please note that the slip could be a vector

- Two choices: for each sub-fault,
  Linear formulation: slip time series $\longrightarrow$ thousands of unknowns.
  Non-linear formulation: defined by few parameters (rupture time, peak and rise times)
- Non-linear formulation: favorite approach $\rightarrow$ Why?

  few seismograms per earthquake

♦ Time approach for 1979 Imperial Valley quake (Hartzell and Heaton, 1983; Archuleta, 1984)

♦ Frequency approach (low/high hierarchy) for 1992 Landers quake (Cotton and Campillo, 1995)

Both strategies have difficulties ...

No unique solution!

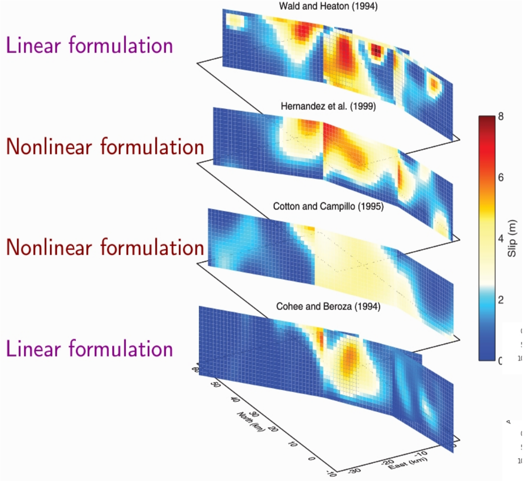

Variability of earthquake source models
(from Minson et al. 2013)

VARIABILITY AMONG SOLUTIONS FOR THE SAME EARTHQUAKE!

Which of them is the good one?

Linear formulation of the kinematic source inversion

With denser and denser seismic networks around active faults,
linear inversion has attracted more and more interest both in frequency (Fan et al., 2014) and in time (Somala et al., 2014).

Spatio-temporal slip vector on fault plane (dip and strike directions).

⧫ Frequency approach:

- Possible negative slip-rate.
- Challenging integration of prior rupture physics.

⧫ Time approach:

- Slip-rate positivity honored.
- Prior rupture physics, such as sparsity (Heaton, 1990) and causality (Olson and Apsel, 1982).

Objective of our kinematic inversion scheme

Spatio-temporal slip-rate inversion
through linear formulation

Adjoint-state method for getting the gradient when considering a linear formulation.

Model parameters: two slip-rate components over planar subfaults defined by a normal $\underline{n}$

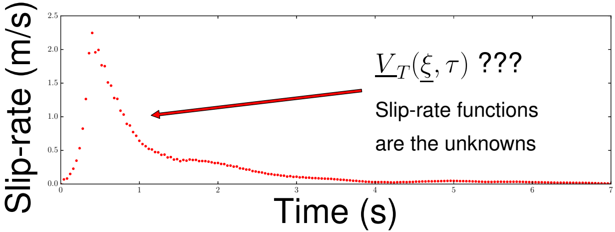

Slip-rate component on each subfault

Contributions:

- Adjoint formulation and necessary regularization
- Benchmark illustration
- Real earthquake application
- Time-evolution reconstruction using causality.

Misfit function of a linear forward problem

- Least-squares misfit function (convex quadratic function): sum of squared sample differences of observed and synthetic seismograms.

$$\mathcal{C}(\underline{V}_T) = \frac{1}{2}\int_{t_1}^{t_2} (\underline{v}-\underline{u})^T \underline{\underline{W}}^T \underline{\underline{W}}(\underline{v}-\underline{u})dt$$

with observed seismograms $\underline{u}$ and data covariance matrix $\underline{\underline{W}}$ often taken as diagonal matrix.

- Constrained local optimization using the gradient of the misfit function.

$$\min_{\underline{V}_T} \quad \mathcal{C}(\underline{V}_T) = \frac{1}{2}\int_{t_1}^{t_2} (\underline{v}-\underline{u})^T \underline{\underline{W}}^T \underline{\underline{W}}(\underline{v}-\underline{u})dt,$$

$$\text{s. t.} \quad \underline{F}(\underline{x},t) = v_n(\underline{x},t) - \sum_i \int_{t_1}^{t_2} d\tau \int\int_{\underline{\xi}} V_{T_i}(\underline{\xi},\tau)\mathcal{T}_{ni}(\underline{\xi},t-\tau;\underline{x},0)d\underline{\xi} = 0.$$

Two options:

1. Adjoint-state method (simple & efficient), (Plessix, 2006)
2. Fréchet derivatives (more computationally expensive but affordable)

Gradient computation

Adjoint-state field $\underline{\hat{\lambda}}$: residuals between synthetic and observed seismograms:

$$\underline{\hat{\lambda}}(\underline{x}, t) = \underline{\underline{W}}^T \underline{\underline{W}} \left(\underline{v}(\underline{x}, t) - \underline{u}(\underline{x}, t) \right),$$

Misfit gradient $\underline{\mathcal{G}}$: convolution between residuals and stress-state $\mathcal{T}_{ni}$

$$\mathcal{G}_i(\underline{\xi}, \tau) = \sum_{\underline{x}} \sum_{n=1}^{3} \int_{\tau_1}^{\tau_2} \hat{\lambda}_n(\underline{x}, t) \mathcal{T}_{ni}(\underline{\xi}, \tau - t; \underline{x}, 0) d\tau,$$

$$(n \in \{1, 2, 3\} \text{ and } i \in \{1, 2\})$$

Two components to be recovered on the fault plane: they define the rake angle.

1: **Require** fault plane & acquisition definition and pre-computed stress state

2: **Input** observations: 3-C seismograms at each receiver

3: **Initialize** the slip-rate $\underline{\hat{V}}^k_T(\underline{\xi}, \tau) = \underline{0}$, $k = 1$

4: **while** *convergence is not reached* **do**

- 4.1: Compute $\underline{\hat{v}}^k(\underline{x}, t)$ (forward modeling) with $\underline{\hat{V}}^k_T(\underline{\xi}, \tau)$
- 4.2: Estimate residuals, $\underline{\hat{\lambda}}^k(\underline{x}, t) = \underline{\hat{v}}^k(\underline{x}, t) - \underline{u}(\underline{x}, t)$
- 4.3: Calculate the gradient using the residuals

$$\mathcal{G}^k_i(\underline{\xi}, \tau) = \sum_{\underline{x}} \sum_{n=1}^{3} \int_{\tau_1}^{\tau_2} \hat{\lambda}^k_n(\underline{x}, t) \mathcal{T}_{ni}(\underline{\xi}, \tau - t; \underline{x}, 0) dt$$

- 4.4: Update the slip-rate $\underline{\hat{V}}^{k+1}_T = \underline{\hat{V}}^k_T + \alpha^k \Delta \underline{\hat{V}}^k_T(\underline{\mathcal{G}}^k)$, $k = k + 1$

end

Algorithm 1: Kinematic source inversion using the adjoint-state method.

Few data: how to reduce the size of the null space

Linear time formulation leads to a significant number of parameters

Full data window
(total time window)

- Rupture time regularization
- Boundary condition for vanishing slip-rate
- Spatial coherence of slip distribution

Increasing data window
(work in progress)

- Same items as for full window ... and
- Progressive assimilation of the new data to be explained
- Prediction of the new slip

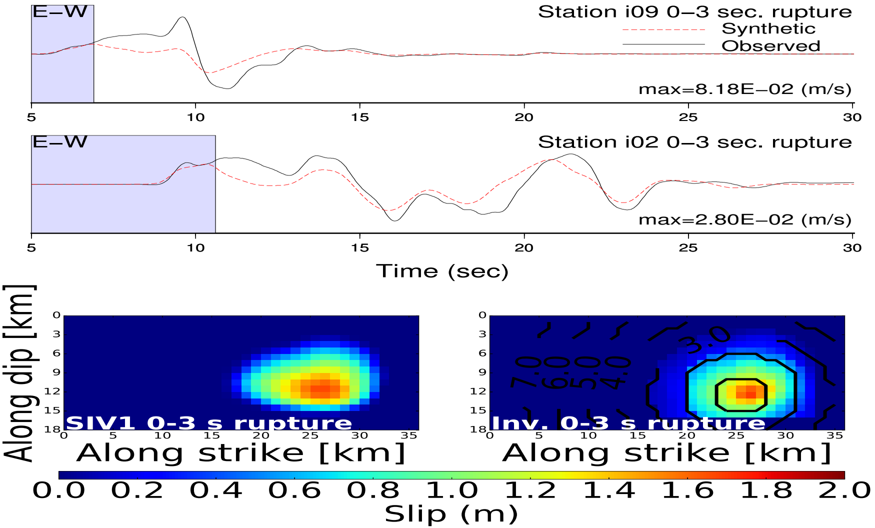

Target at 3 seconds

Inversion first data time window

Too few data: regularization based on prior information and preconditioning

Null space can be quite large (reason for model reduction)

Regularization needed for linear time formulation:

- data term strategy: model preconditioning through smoothing data gradient
- model term strategy: emphasizing smooth model and
  adding model gradient (prior model and model covariance)

$$\mathcal{C}(\underline{V}_T) = \mathcal{C}_d(\underline{V}_T) + \mathcal{C}_{1m}(\underline{V}_T) + \mathcal{C}_{2m}(\underline{V}_T)$$

$\mathcal{C}_d(\underline{V}_T) \longrightarrow$ Data misfit term

$\mathcal{C}_{1m}(\underline{V}_T) \longrightarrow$ Tikhonov model regularization term

$\mathcal{C}_{2m}(\underline{V}_T) \longrightarrow$ model misfit term

2D smoothing gaussian filter applied to the data gradient

Diagonal model covariance design based on expected rupture physics

Prior model design based on expected rupture physics

Model misfit function based on prior model $\underline{V}_{T_0}$ and weighted matrix $\underline{\underline{W}}_R$

$$\mathcal{C}_{2m}(\underline{V}_T) = \frac{1}{2}\int_{\tau_2}^{\tau_1} (\underline{V}_T - \underline{V}_{T_0})^T \underline{\underline{W}}_R^T \underline{\underline{W}}_R (\underline{V}_T - \underline{V}_{T_0}) d\underline{\tau}$$

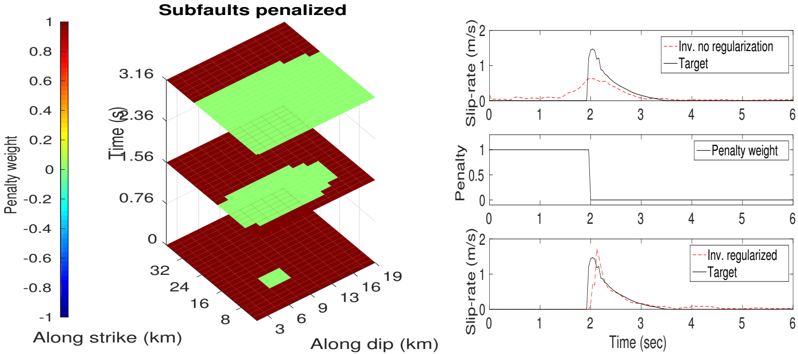

Penalizing effect of designing $\underline{\underline{W}}_R$.

Rupture could not occurred before a given time in this example.

Possible to prevent future slip after a given time

(Asnaashari et al., 2013)

Various prior model and covariance matrices promoting rupture physics:

- Rupture causality (time-space model penalization).
- Penalized slip at boundaries (discouraging infinite strain).
- Neighbouring coherence of temporal rupture over close subfaults.

Remark: many suggestions of promoting possible dynamic ruptures

Time for verification exercises ...

Questions / goals:

- Does it work for realistic configuration?
- Does it work for real data?
- How to design model-driven component?
- How far are the results from the true solution?

???

Outline

Fault plane geometry:

Strike $= 90^o$, dip $= 80^o$, rake $= 90^o$

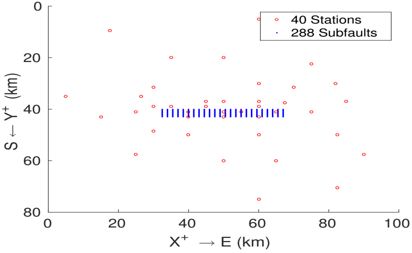

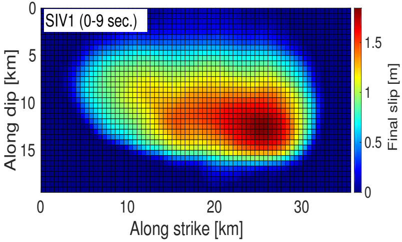

Expected final slip

Medium structure

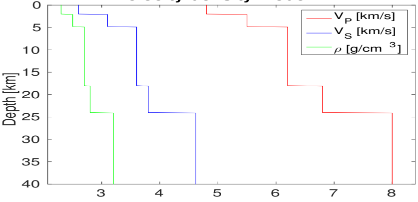

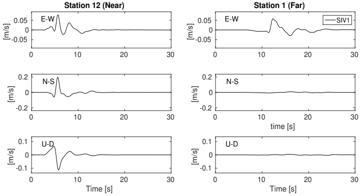

Data: 40 receivers

(Mai et al., 2016)

SIV1 results from other teams: still strong variability!

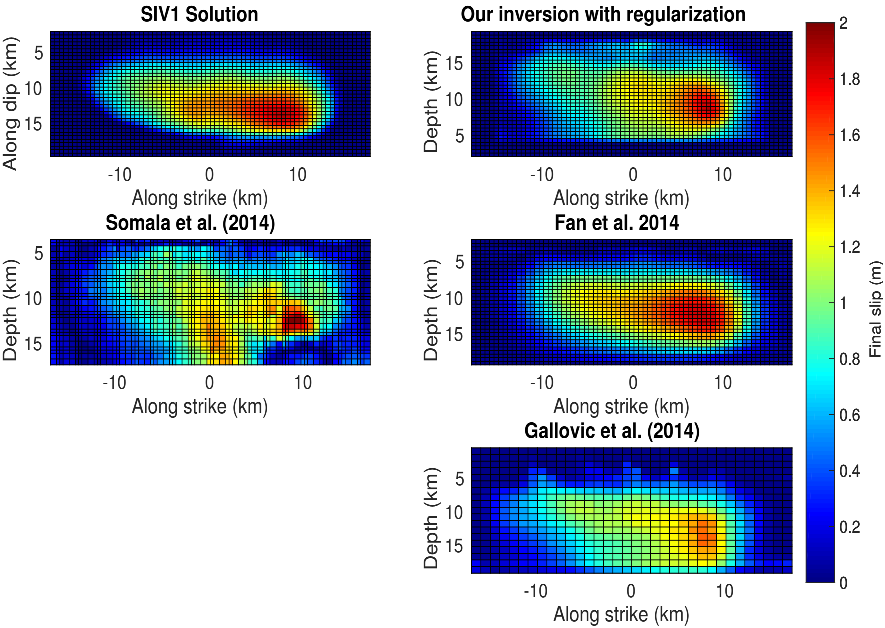

Our inversion (time domain)

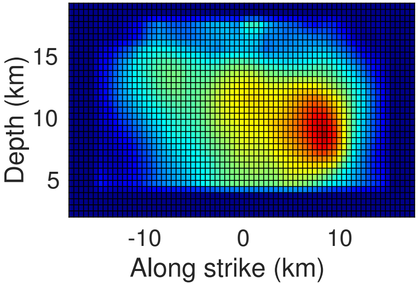

Fan et al. 2014 (frequency domain)

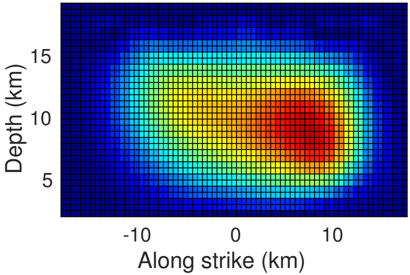

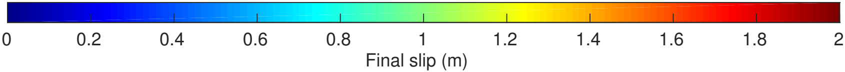

Time

- Simple design of regularization
- Positivity of the solution
- Causality enforced in # ways

Frequency

- low to high frequencies
- Indirect constraints
- Causality not ensured

In frequency, slip-rate could be negative!

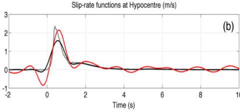

Outline

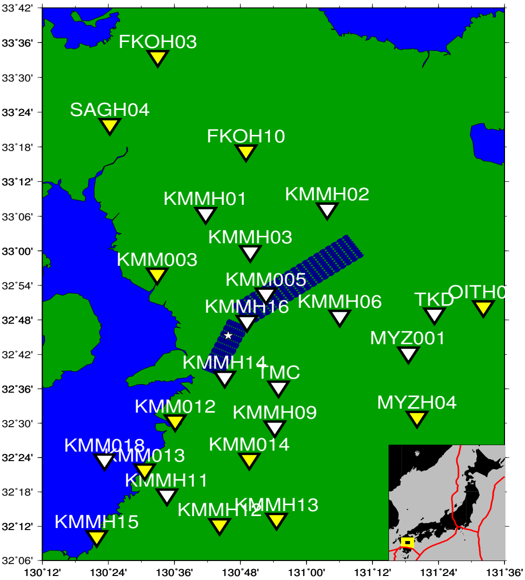

There are two fault segments:

- strike 205^o, dip 72^o
- strike 235^o, dip 65^o

Well recorded earthquake!

- 30 traces EW
- 30 traces NS
- 30 traces UD

(Asano and Iwata, 2016; Uchide et al., 2016)

Uchide et al. (2016)
17 stations used

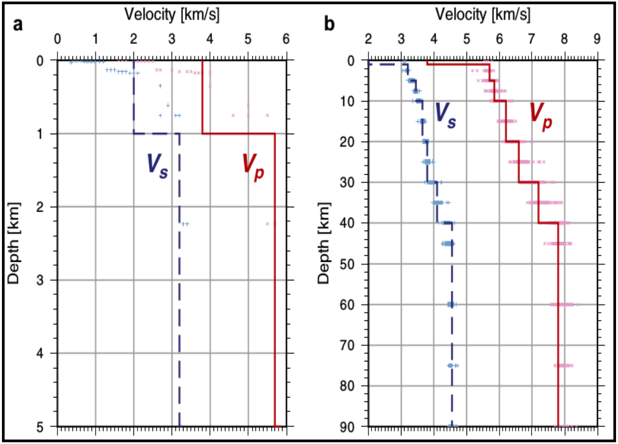

After checking our dataset, the velocity structure on the right is preferred.

An added hierarchical workflow for rake determination

1: Select few high-quality stations and run a first inversion with no regularization and no prior information: Invert for the slip-rate vector (2 components).

2: Detect the rake angle (relation between the two vector components).

3: Fix the rake angle and invert for the amplitude of the slip-rate vector.

4: Identify the rupture velocity by analysing the propagating slip-rate pulses.

5: Set the required regularization terms using the knowledge from previous inversions to perform the last inversion.

Algorithm 2: Hierarchical workflow to include prior information, such as the rake angle or the expanding rupture front.

Uchide et al. (2016)

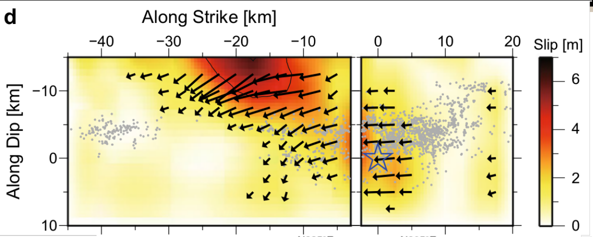

Asano and Iwata (2016)

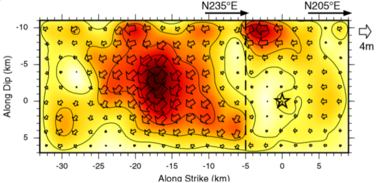

Similarities

- 1^{rst} segment strike-slip
- 2^{nd} segment strike-dip-slip
- Maximum slip $\approx$ 18 km to the East from hypocenter

Differences

- Depth of maximum slip patches (different dataset/dip resolution)
- Number of patches
- Fault length

2016 Kumamoto earthquake: slip-rate vector inversion

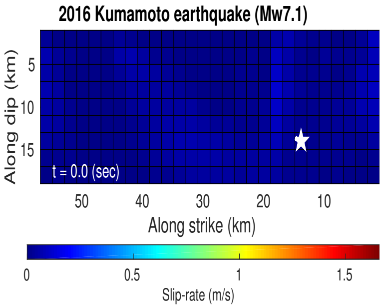

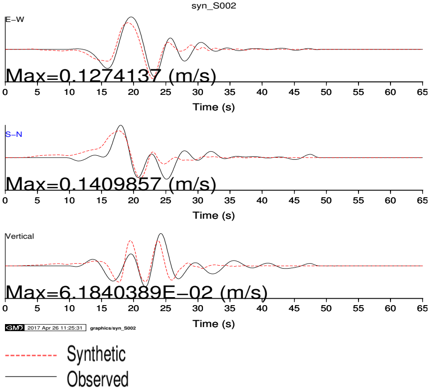

Model regularization design and model preconditioning not enough!

Non-physical effects still exist.

Decent results by smoothing the gradient and enforcing rupture causality.
Rake angle extracted from an initial inversion is fixed for the final inversion.

Our solution

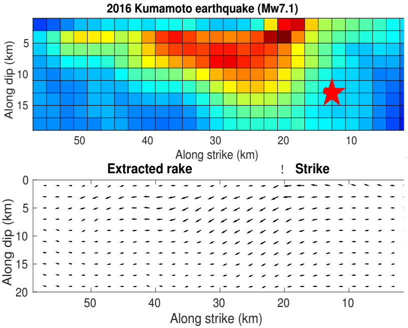

Uchide et al. (2016)
Asano and Iwata (2016)

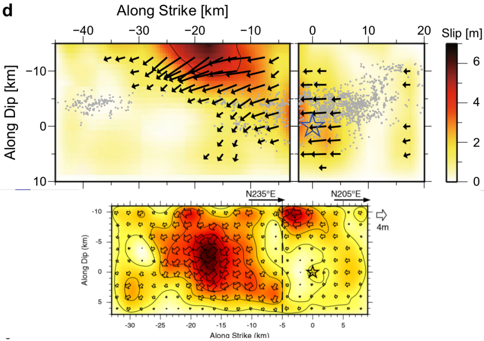

Complex slip-rate functions.

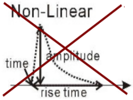

Examples over few sub-faults

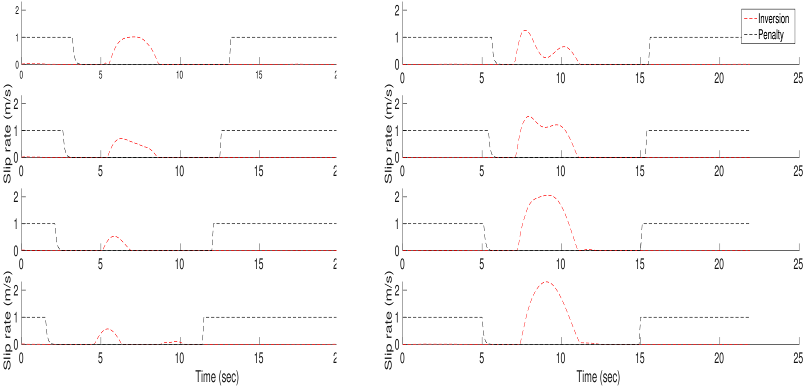

Slip-rate time history different from triangular shape function (model reduction strategy)!

Outline

Causality through a time progression of providing the data?

Available precomputed stress-state, $\mathcal{T}_{ni}(\underline{\xi}, t-\tau; \underline{x}, 0)$, has wave propagation information and, therefore, time window relation between source points and receivers!

$$v_n(\underline{x}, t) = \sum_i \int_{t_1}^{t_2} d\tau \int \int_{\underline{\xi}} V_{T_i}(\underline{\xi}, \tau)\mathcal{T}_{ni}(\underline{\xi}, t-\tau; \underline{x}, 0) d\underline{\xi}.$$

$$\mathcal{G}_i(\underline{\xi}, \tau) = \sum_{\underline{x}} \sum_{n=1}^{3} \int_{\tau_1}^{\tau_2} \hat{\lambda}_n(\underline{x}, t)\mathcal{T}_{ni}(\underline{\xi}, \tau - t; \underline{x}, 0) d\underline{\xi}.$$

Reminder:

$\underline{\hat{\lambda}} \longrightarrow$ residuals

$\underline{v} \longrightarrow$ synthetics

$\underline{u} \longrightarrow$ observations

$\underline{\mathcal{G}} \longrightarrow$ Gradient

$\underline{V}_T \longrightarrow$ Slip-rate (unknowns)

- Existing relation between data time windows and source time-space windows.
- Causality is enforced drastically by data prediction

(in addition to model constraints).

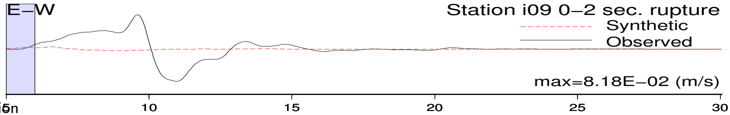

Data time windowing strategy for progressive model increase

Data time-windows:
We assume that the first arrivals can only come from the nucleation zone. Then, Green's functions and forward modeling can be used to establish the limited data time-window of each record used to invert for a specific model time-space windows.

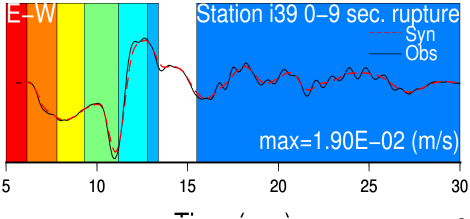

Model time-space-windows:
Considering as known the hypocentral location and the origin time when the rupture starts, expected zones and time intervals where to perform slip-rate inversion are known. These areas and time intervals are estimated through an Eikonal solver. Only an maximum upper bound of the rupture velocity is assumed.

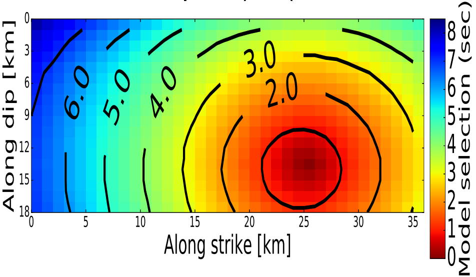

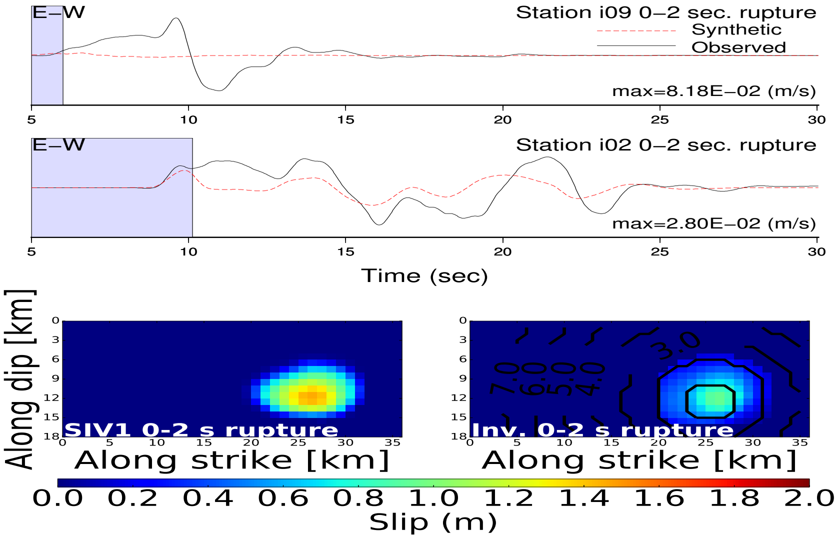

We increment the next solution from the previous one while still accepting modifications where the rupture has already occurred.

Outline

Real data application?

- Improve rake estimation and regularization for 2016 Kumamoto earthquake
- Apply time progressive strategy to 2016 Kumamoto earthquake
- Assessment of uncertainties, thanks to the linearity of the forward problem
- Write down all what I have found.

Room for improvements

- Linear formulation in the time domain with simple regularization terms shows promising advantages.
- Complex reconstruction of the slip history is expected if acquisition density increases.
- Rake constraint helps to focus the energy in the correct direction and at the right time.
- Time progressive strategy integrates causality in a better way (synthetic illustration).

Thanks for listening

(Please let me know about possible improvements)

Acknowledgements

Many thanks to:

- Centre National de la Recherche Scientifique, CNRS (PhD scholarship)
- Université Grenoble Alpes, UGA
- Institut des Sciences de la Terre, ISTerre
- Consortium SEISCOPE
- ANR S4 "Subduction: Standard and Slow Seismology"
- Universidad Nacional Autonoma de Mexico, Facultad de Ingenieria, FI
- Universidad Nacional Autonoma de Mexico, Instituto de Geofisica, IGEOF

Aki, K. and Richards, P. G. (2002). *Quantitative seismology, theory and methods, second edition*. University Science Books, Sausalito,California.

Archuleta, R. J. (1984). A faulting model for the Imperial Valley earthquake. *Journal Geophysical Research*, 89:4559–4585.

Asano, K. and Iwata, T. (2016). Source rupture processes of the foreshock and mainshock in the 2016 kumamoto earthquake sequence estimated from the kinematic waveform inversion of strong motion data. *Earth, Planets and Space*, 68(1):147.

Asnaashari, A., Virieux, J., Garambois, S., and Audebert, F. (2013). *Quantitative 4D seismic imaging in complex media using 2D full waveform inversion*. PhD thesis, PhD thesis: Université de Grenoble.

Beresnev, I. A. (2003). Uncertainties in finite-fault slip inversions: to what extent to believe?(a critical review). *Bulletin of the Seismological Society of America*, 93(6):2445–2458.

Cotton, F. and Campillo, M. (1995). Frequency domain inversion of strong motions: Application to the 1992 landers earthquake. *Journal of Geophysical Research: Solid Earth*, 100(B3):3961–3975.

Fan, W., Shearer, P. M., and Gerstoft, P. (2014). Kinematic earthquake rupture inversion in the frequency domain. *Geophysical Journal International*, 199(2):1138.

Hartzell, S. H. and Heaton, T. H. (1983). Inversion of strong ground motion and teleseismic waveform data for the fault rupture history of the 1979 imperial valley, california, earthquake. *Bulletin of the Seismological Society of America*, 73(6A):1553–1583.

Heaton, T. H. (1990). Evidence for and implications of self-healing pulses of slip in earthquake rupture. *Physics of the Earth and Planetary Interiors*, 64(1):1–20.

Ide, S. (2007). Slip inversion-4.07.

Mai, P. M., Schorlemmer, D., Page, M., Ampuero, J.-P., Asano, K., Causse, M., Custodio, S., Fan, W., Festa, G., Galis, M., et al. (2016). The earthquake-source inversion validation (siv) project. *Seismological Research Letters*.

Minson, S., Simons, M., and Beck, J. (2013). Bayesian inversion for finite fault earthquake source models i—theory and algorithm. *Geophysical Journal International*, 194(3):1701–1726.

Olson, A. H. and Apsel, R. J. (1982). Finite faults and inverse theory with applications to the 1979 imperial valley earthquake. *Bulletin of the Seismological Society of America*, 72(6A):1969–2001.

Somala, S. N., Ampuero, J.-P., and Lapusta, N. (2014). Resolution of rise time in earthquake slip inversions: Effect of station spacing and rupture velocity. *Bulletin of the Seismological Society of America*.

Uchide, T., Horikawa, H., Nakai, M., Matsushita, R., Shigematsu, N., Ando, R., and Imanishi, K. (2016). The 2016 kumamoto–oita earthquake sequence: aftershock seismicity gap and dynamic triggering in volcanic areas. *Earth, Planets and Space*, 68(1):180.

Synthetic circular rupture test for checking illumination

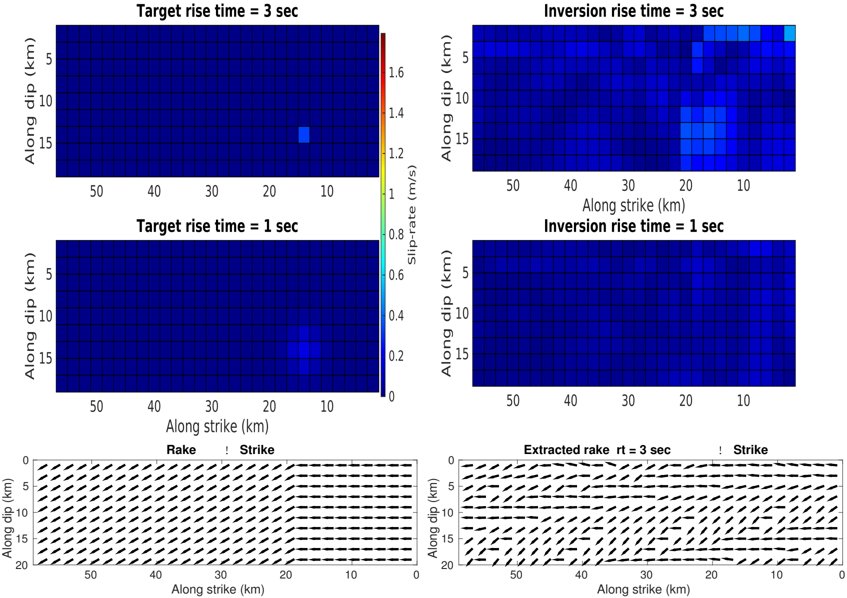

1-step inversion using $\approx H^{-1}$ (7000/16416 singular values)

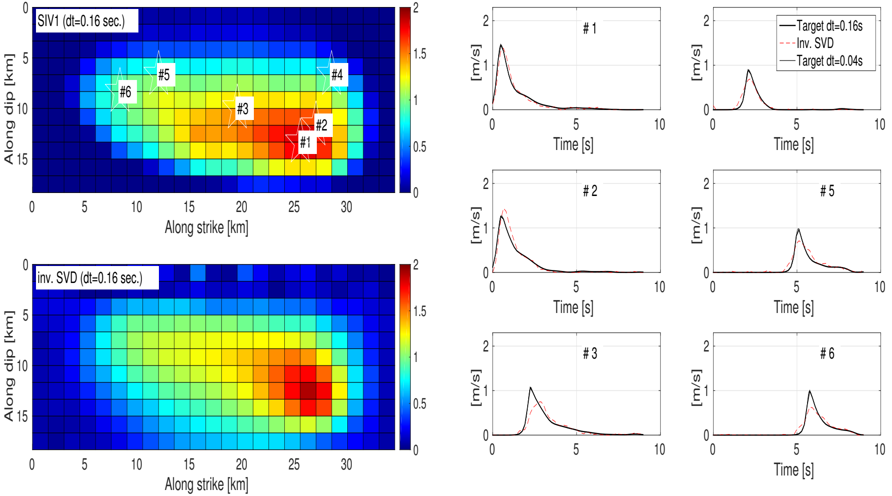

Model misfit function based on prior model $\underline{V}_{T_0}$ and weighted matrix $\underline{\underline{W}}_R$

$$\mathcal{C}_{2m}(\underline{V}_T) = \frac{1}{2} \int_{\tau_2}^{\tau_1} (\underline{V}_T - \underline{V}_{T_0})^T \underline{\underline{W}}_R^T \underline{\underline{W}}_R (\underline{V}_T - \underline{V}_{T_0}) d\underline{\tau}$$

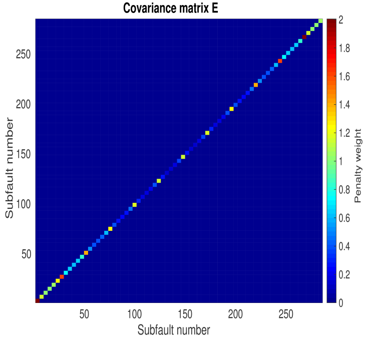

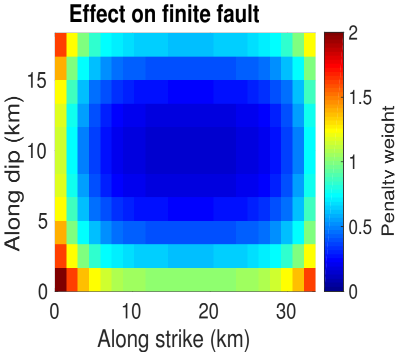

Penalizing effect of designing $\underline{\underline{W}}_R$.

Penalizing effect at the edges of the fault for slip-rate estimation.

Avoid infinite strain at the edges of the rupture (Beresnev, 2003).

Model misfit function based on prior model $\underline{V}_{T_0}$ and weighted matrix $\underline{\underline{W}}_R$

$$\mathcal{C}_{2m}(\underline{V}_T) = \frac{1}{2} \int_{\tau_2}^{\tau_1} (\underline{V}_T - \underline{V}_{T_0})^T \underline{\underline{W}}_R^T \underline{\underline{W}}_R (\underline{V}_T - \underline{V}_{T_0}) d\underline{\tau}$$

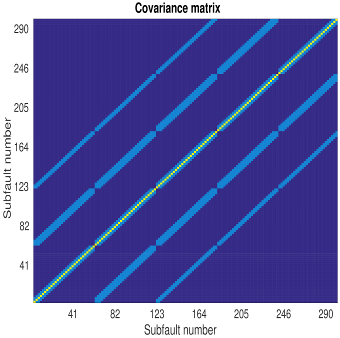

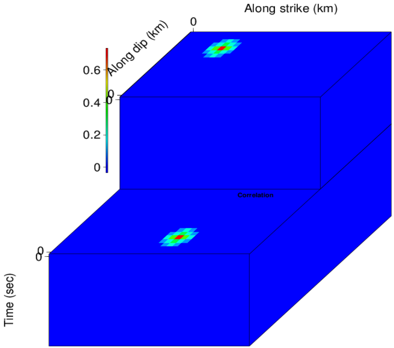

Penalizing effect of $\underline{\underline{W}}_R$.

Spatial coherence: only neighbouring subfaults of a broken subfault (within a given correlation length) are allowed to break.

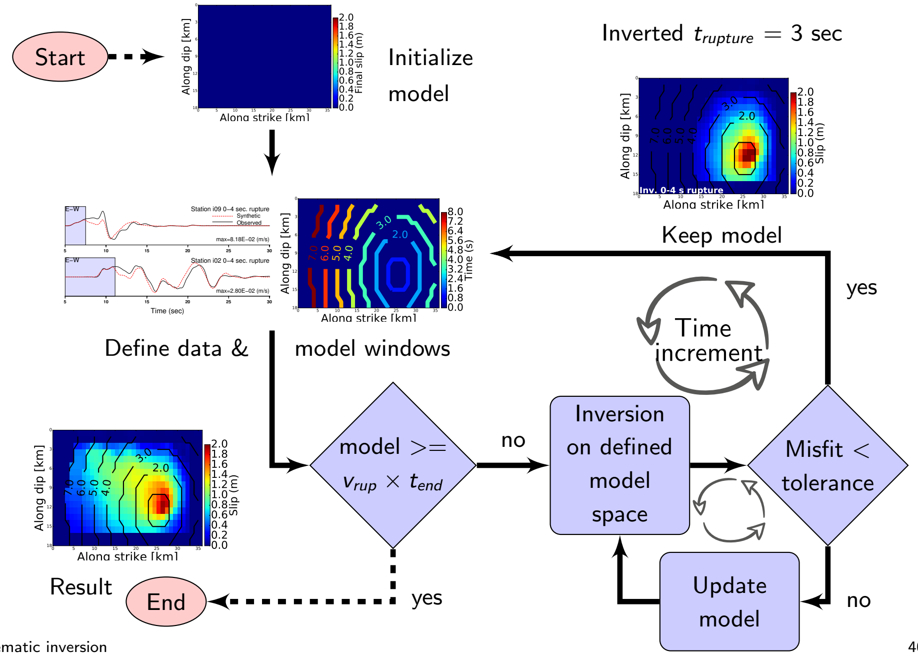

Start
Initialize model
Along dip [km]
Along strike [km]
Final slip (m)
Inverted $t_{rupture}$ = 3 sec
Slip (m)
Inv. 0-4 s rupture
Keep model
Station i09 0–4 sec. rupture
Synthetic
Observed
max=8.18E−02 (m/s)
Station i02 0–4 sec. rupture
max=2.80E−02 (m/s)
E–W
Time (sec)
Time (s)
yes
Time increment
Define data & model windows
model $>=$ $v_{rup} \times t_{end}$
no
Inversion on defined model space
Misfit $<$ tolerance
Result
End
yes
Update model
no

Asano and Iwata (2016), 15 stations

Local distance

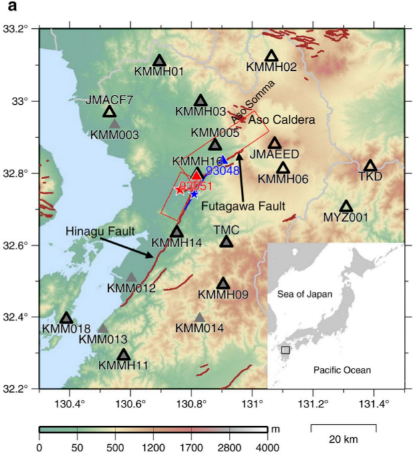

Uchide et al. (2016) 17 stations

Regional distance